IL NUOVO CIMENTO **42 C** (2019) 17
DOI 10.1393/ncc/i2019-19017-x

Colloquia: SoHe3 2018

Numerical simulations of high cross-helicity turbulence from 0.2 to 1 AU

A. Verdini([1]), R. Grappin([2]), V. Montagud-Camps([2]), S. Landi([1]), L. Franci([3]) and E. Papini([1])

([1]) *Dipartimento di Fisica e Astronomia, Universitá di Firenze - Firenze, Italy*
([2]) *LPP, Ecole Polytechnique - Palaiseau, France*
([3]) *Schoool of Physics and Astronomy, Queen Mary University of London - London, UK*

received 28 December 2018

Summary. — Turbulence in the fast stream of the solar wind is maintained despite the small compressibility and a dominance of outward-propagating fluctuations ($z^+ > z^-$), in contrast to its rapid decay in imbalanced homogenous MHD turbulence. We numerically study if the inhomogeneity introduced by solar wind expansion can be an effective source of z^- that maintains turbulence. Starting at 0.2 AU with $z^- = 0$, we obtain a damping with distance of z^+ and a quasi-steady level of z^-. The z^+ spectrum steepens with distance toward a -1.4 power-law at 1 AU, while the z^- spectrum has a $-5/3$ power-law index at all distances. These properties are robust against variations of the input spectrum and expansion rate and are in agreement with *in-situ* data, suggesting that imbalanced turbulence can be maintained by expansion alone.

1. – Introduction

Solar wind offers the closest example of a wind tunnel with turbulence at large Reynolds. For scales larger than proton scales, Magnetohydrodynamics (MHD) is an accepted framework to describe nonlinear dynamics in a plasma. Among the important open questions, the case of Alfvénic turbulence in fast streams, *i.e.* with large cross-helicity and weak compressibility, has been early noted to be paradoxical [1]. Because of the large cross-helicity, the outward fluctuations are much stronger than the inward one, $z^+ >> z^-$, so that one expects nonlinear couplings to be progressively depleted, leading to the switch off of turbulence. However, a turbulent cascade seems to be well alive, since well-developed spectra are observed on several decades of frequencies for all explored distances from the Sun, $R > 0.3\ AU$, *e.g.* [2, 3].

In order to sustain turbulence one needs to inject z^- that otherwise will be rapidly damped leading to vanishing nonlinear interaction [1]. This can be done via shear interaction between fast and slow streams [4, 5], parametric instability of large amplitude Alfvén

Creative Commons Attribution 4.0 License (http://creativecommons.org/licenses/by/4.0)

waves (*e.g.* [6]), or solar wind expansion [7]. Observational constraints [8-12] can help in understanding which mechanism is actually at work in fast streams. For Alfvénic turbulence: (i) the sub-dominant species has a remarkable constancy in its level and spectral slope at all distances (background spectrum)' (ii) the cross-helicity must decrease with heliocentric distance, its variation being mainly due to the fall of the dominant species; iii) at 1 AU the spectrum of the dominant species is flatter than the spectrum observed in non-Alfvénic streams, having a slope close to $-3/2$ instead of $-5/3$. Despite shear interaction is able to reproduce some of the above properties, its importance is largely reduced in the polar wind that is composed of fast streams only. Also, parametric instability can account for the decay of cross helicity, but the resulting spectra are too steep compared to observations [13]. Expansion has not been tested against observations. In this work we numerically study the sustainment of turbulence in the expanding solar wind using the Expanding Box Model (EBM) that includes expansion in the 3D MHD equations [14-18]. We consider a plasma volume placed initially at the distance of 0.2 AU with a spectrum of purely outgoing Alfvén species and follow the development of turbulence as it is advected by the wind.

2. – Method

We use the EBM to simulate 3D MHD turbulence in a periodic domain whose size is smaller than the initial heliocentric distance, $(L_r,\ L_{tr}) << R_0$, where the subscripts $r,\ tr$ indicate directions parallel and transverse to the radial one. As time proceeds, the domain is advected by the solar wind at constant speed U_0 moving to larger distances, $R = R_0 + U_0 t$, while it expands anisotropically, $L_r = const$ and $L_{tr} \propto R$. The EBM equations are very similar to the primitive MHD equations and their complete form can be found in [14, 19]. We recall that an additional non-dimensional parameter is introduced, the expansion parameter, defined as,

$$e = \frac{t^0_{NL}}{t^0_{exp}} = \frac{U_0/R_0}{u_{rms}k^0_{tr}}, \tag{1}$$

which is basically the inverse of the age of turbulence [20] at the initial position. Note that the expansion and advection times are equal, $t_{ad} = t^0_{exp} = R_0/U_0$, and the nonlinear time $t^0_{NL} = (k^0_{tr} u_{rms})^{-1}$ is build on the largest scale transverse to the radial direction, $k^0_{tr} = 2\pi/L_{tr}$.

We initialize the simulations with a superposition of outward-propagating Alfvénic fluctuations with random phases, rms values $z^+_{rms} = 2$, and equipartition between the magnetic and (divergence-free) velocity fluctuations, $u_{rms} = b_{rms} = 1$ and $\boldsymbol{\nabla}\cdot\boldsymbol{u} = 0$. The initial spectrum is strongly anisotropic, denoting with $k_\parallel$ and $k_\perp$ the wavevectors parallel and perpendicular to the mean field, $B_0 \sim 2$, the energy isocontours have an aspect ratio equal to that one of the (anisotropic) domain, $k_\perp/k_\parallel = L_r/L_{tr} = 5$. The initial temperature is large to maintain small turbulent Mach numbers, $M = u_{rms}/c_s \sim 1/8$ (the plasma $\beta \sim 20$ is also not realistic), and all simulations have a resolution of 512 points in each direction. We start at the initial position $R_0 = 0.2$ AU with a mean magnetic field at an angle of 11^o with the radial direction, and we let the system evolve until $5R_0 = 1$ AU where B_0 has an angle of 45^o.

In order to explore the conditions for the sustainment of the turbulent cascade, we will vary three parameters, the expansion parameter $e \in [0.1, 2]$, the cutoff $k_{cut} \in [4, 64]$, and the slope $p \in [-3, -1]$ of the the initial spectrum. By varying the the expansion

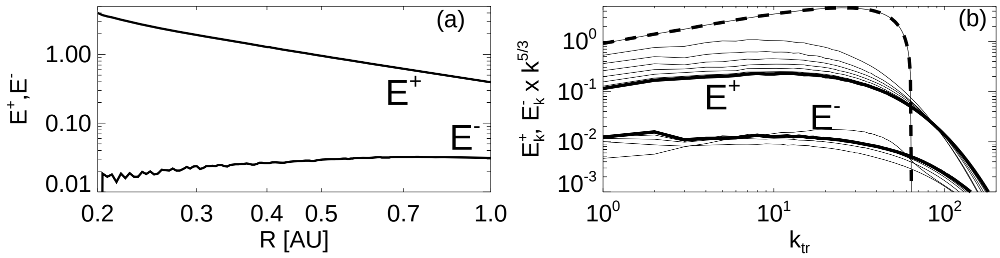

Fig. 1. – (a) Energy of the Elsasser species, $E^{\pm}$, versus distance for parameters $e = 0.1$, $k_{cut} = 64$, $p = -1$. (b) One dimensional spectra in the transverse wavenumber, k_{tr}, compensated by 5/3 at distances between 0.2 AU (dashed line) and 1 AU (thick lines).

parameter we can roughly set how many eddy-turnover times elapse before reaching 1 AU. By decreasing the initial cutoff or increasing the initial slope, we can reduce the energy contained in those (large) wavenumbers for which $t_{NL}(k) << t_{exp}$ and so reduce the initial turbulence activity.

3. – Results and Discussion

In figure 1(a) we plot the Elsasser energies $E^{\pm} = |z^{\pm}|^2$ as a function of distance for $k_{cut} = 64$, $p = -1$, $e = 0.1$, that is, parameters that maximize the turbulent activity. The energy in the outward fluctuation decreases steadily, while that one of the inward fluctuations increases from its initial zero value and saturates beyond 0.5 AU. This behaviour is opposite to that one of dynamic alignment (E^+ is constant, E^- decreases) and consistent with observations. However, the decay of cross helicity is modest because $E^+ > 10E^-$ at all distances. In figure 1(b) we plot the one-dimensional spectra of $E^{\pm}$ as a function of the transverse wavenumber k_{tr} at several distances and compensated by $k^{5/3}$. The spectrum of E^+ decreases while steepening with distance and attains an asymptotic slope that is flatter than$-5/3$. On the contrary, after an initial growth, the E^- spectrum is extremely stable, maintaining the same energy and the same slope (very close to $-5/3$) at all distances, such stability being reminiscent of the observed "background" spectrum.

In fig. 2 we plot the normalized transverse spectra $\tilde{E}^{\pm}(k\eta)$, averaged between $0.9 - 1$ AU and compensated by $k^{5/3}$ (top and bottom rows respectively), for simulations with different expansion parameters (left panel), initial cutoffs (middle panel), and initial slopes (right panel). Before averaging, at each position we use the energy dissipation, $\epsilon_{\pm} = \nu \sum_k k^2 E^{\pm}(k)$, and the viscous- and resistive-coefficient ν to normalize spectra and wavenumbers, $\tilde{E}^{\pm}(k\eta^{\pm}) = E^{\pm}/(\epsilon_{\pm}\nu^5)^{1/4}$, with the dissipation scale being $\eta_{\pm} = (\nu\epsilon^3_{\pm})^{1/4}$ [21, 22]. Styles have been attributed, following the ordering of the parameter values at the top of each figure: solid, dotted, dashed, dot-dashed. The wavenumber intervals in which $E^{\pm}$ spectral slopes can be identified are $k\eta \in [0.007, 0.03]$ and $k\eta \in [0.02, 0.07]$ for $E^{\pm}$, respectively.

Let us consider increasing the expansion parameter (left column). For the smallest expansion ($e = 0.1$) already shown in fig. 1, we find $E^+ \sim k^{-1.5}$ and $E^- \sim k^{-5/3}$. For the strongest expansion ($e = 2$, dashed line), E^+ is flatter and E^- is steeper. As a rule, as expansion increases, the difference in slope between E^+ and E_- increases with E^+ becoming flatter and E^- steeper.

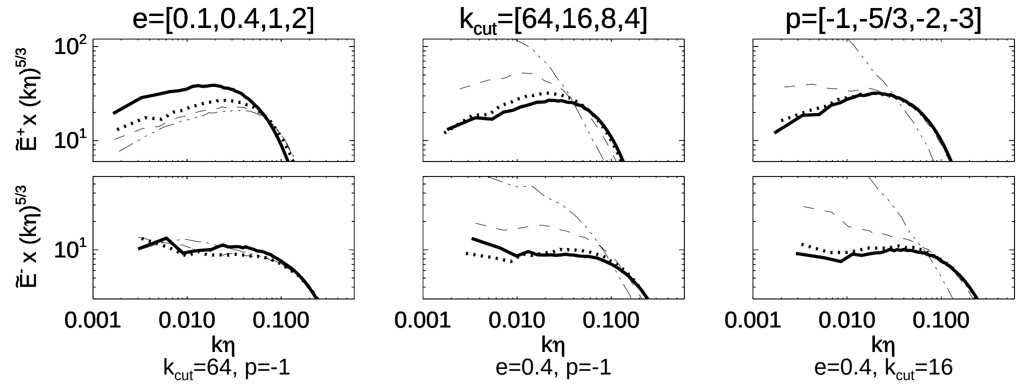

Fig. 2. – Compensated, normalized, averaged one-dimensional spectra of $\tilde{E}^+$ (top) and $\tilde{E}^-$ (bottom) versus normalized transverse wavenumber (see text) for three groups of simulations in which we increase the strength of expansion (thick solid, thick dotted, dashed, dotted-dashed lines) by varying the expansion parameter e, the initial cutoff k_{cut}, and the initial slope p (left, middle, and right columns), while keeping fixed the parameters indicated on the bottom.

We now decrease the cutoff wavenumber from 64 to 4, with slow expansion and initial flat slope (central column). It is seen that too small cutoffs prevent turbulence from developing, thus leading to very steep spectra, while reasonably large values allow convergence to the previously noted couple: flat E^+ and $E^- \sim k^{-5/3}$. We obtain similar results by considering steeper and steeper initial spectra (right column). Here the case $p = -2$ (dashed lines) is interesting because it clearly shows the development of a turbulent cascade for E^+: the spectrum at 1 AU has $E^+ \sim k^{-5/3}$ which is flatter than that one at 0.2 AU.

We have shown that in presence of expansion an *anisotropic* spectrum of outwardly propagating fluctuations evolves into well-developed turbulence provided one starts with a moderate excitation of small wavenumbers, *i.e.*, $k_{cut} > 8$, $p > -2$. When satisfying these conditions, the properties of turbulence converge to the following ones: (i) inward fluctuations that are generated by expansion maintain a constant energy and power-law index $E^- \sim k^{-5/3}$ for $R > 0.5\ AU$; (ii) the energy of outward fluctuations decreases with distance because of expansion and turbulent damping; (iii) at 1 AU the spectrum of the dominant species is flatter than that one of the subdominant species, $E^+ \sim k^{-1.4}$ and $E^- \sim k^{-5/3}$. These properties are in agreement with observations and suggest that turbulence in the polar wind is driven by expansion.

REFERENCES

[1] Dobrowolny M., Mangeney A. and Veltri P., *Phys. Rev. Lett.*, **45** (1980) 144.
[2] Coleman P. J. J., *Astrophys. J.*, **153** (1968) 371.
[3] Bruno R. and Carbone V., *Living Reviews in Solar Physics*, **10** (2013) 2.
[4] Roberts D. A., Ghosh S., Goldstein M. L. and Matthaeus W. H., *Phys. Rev. Lett.*, **67** (1991) 3741.
[5] Roberts D. A., Goldstein M. L., Matthaeus W. H. and Ghosh S., *J. Geophys. Res.*, **97** (1992) 17.
[6] Del Zanna L., Matteini L., Landi S., Verdini A. and Velli M., *J. Plasma Phys.*, **81** (2015) 325810102.
[7] Velli M., Grappin R. and Mangeney A., *Phys. Rev. Lett.*, **63** (1989) 1807.

[8] Roberts D. A., Goldstein M. L., Klein L. W. and Matthaeus W. H., *J. Geophys. Res.*, **92** (1987) 12023.
[9] Tu C.-Y. and Marsch E., *J. Geophys. Res.*, **95** (1990) 4337.
[10] Bavassano B., Pietropaolo E. and Bruno R., *J. Geophys. Res.*, **105** (2000) 12697.
[11] Bavassano B., Pietropaolo E. and Bruno R., *J. Geophys. Res.*, **105** (2000) 15959.
[12] Chen C. H. K., Bale S. D., Salem C. S. and Maruca B. A., *Astrophys. J.*, **770** (2013) 125.
[13] Malara F., Primavera L. and Veltri P., in proc. of *Solspa 2001*, edited by Sawaya-Lacoste H., Vol. 477 of *ESA Special Publication* 2002, pp. 309–312.
[14] Dong Y., Verdini A. and Grappin R., *Astrophys. J.*, **793** (2014) 118.
[15] Verdini A. and Grappin R., *Astrophys. J. Lett.*, **808** (2015) L34.
[16] Verdini A. and Grappin R., *Astrophys. J.*, **831** (2016) 179.
[17] Grappin R., Müller W.-C. and Verdini A., *Astron. Astrophys.*, **589** (2016) A131.
[18] Montagud-Camps V., Grappin R. and Verdini A., *Astrophys. J.*, **853** (2018) 153.
[19] Grappin R. and Velli M., *J. Geophys. Res.*, **101** (1996) 425.
[20] Grappin R., Velli M. and Mangeney A., *Annales Geophysicae (ISSN 0939-4176)*, **9** (1991) 416.
[21] Gotoh T., Fukayama D. and Nakano T., *Physics of Fluids*, **14** (2002) 1065.
[22] Müller W.-C., Biskamp D. and Grappin R., *Phys. Rev. E*, **67** (2003) 066302.